

THE LOCUS OF FAILURE OF THE INTERPHASE IN GLASS FIBRE COMPOSITES WITH PLASMA POLYMER SIZINGS

Penchom Photjanataree¹, Timothy Swait² and Frank R Jones^{2*}

²Department of Materials Science and Engineering, University of Sheffield, Mappin Street, Sheffield, S1 3JD, UK.

¹Thai Packaging Centre, Thailand Institute of Scientific and Technological Research, Bangkok, Thailand 1090

*f.r.jones@sheffield.ac.uk

Keywords: Interface/Interphase, Plasma polymers, ToF SIMS fractography.

Abstract

The mechanical properties of a structural composite can be optimised by careful control of the properties of the interphase which forms during processing. We have shown elsewhere that plasma polymerisation is a potential gaseous sizing technique which combines conformal coating with functionalisation of the reinforcing fibres. The interlaminar shear strength of high volume fraction composites was shown in a previous paper, to be dependent on the thickness and functionality of the coating. The objective of this study was to identify the locus of interfacial failure and study the penetration of the epoxy resin into the plasma polymer coating during composite fabrication. We have simulated this using a matrix resin with a detectable label so that its interaction with the plasma polymer could be studied. ToF-SIMS imaging of the fracture surfaces of the model composite was carried out to study the interaction of the plasma polymer with the matrix resin to form a model interphase at the glass interface.

1 Introduction

Plasma polymerization is a potential gaseous sizing technique for reinforcing fibres because the functionality of the deposit can be tuned for coupling chemistry to the matrix polymer or resin [1, 2]. Plasma polymerisation provides a conformal nanoscale coating whose chemical structure can be controlled by choice of monomers and deposition conditions. With a low power the functionality in the monomer can be retained in the coating. In this way the reactivity of the sizing can be matched to the matrix resin. However in a previous study, it was postulated that an interphase formed between the plasma polymer (PP) coating on an E-glass fibre and the epoxy resin because the interlaminar shear strength (ILSS) was found to be a function of plasma polymer thickness [3]. Both acrylic acid and allylamine monomers have been used to introduce defined concentrations of carboxyl and amine groups into crosslinked conformal deposits on the fibres. However the thickness-dependence of the PP on ILSS of the composites differed despite the known reactivity of both NH₂ and COOH functional groups in the PP with epoxy groups in the resins. These promote strong chemical covalent bonds between the fibre and matrix resin at the interface. The formation of the chemical bonds between the amine and epoxy groups has been documented by Drzal et al [4]. However, for the fibres coated with the allylamine PP the ILSS was lower than that for the uncoated fibres. A higher interphase modulus could explain the apparent higher stress transfer efficiency between the matrix to the fibre [5]. For the acrylic acid PP copolymer system the ILSS reached that of the unsized fibres when the coating was reduced to 5 nm. However with the allylamine PP extrapolation to a thickness of approximately 2 nm was required. Liu et al. [3]

interpreted these observations as indicating that an interphase formed by the diffusion of the matrix resin into the acrylic acid and allylamine PP copolymers to differing degrees. So that when the penetration length is less than the thickness of the plasma polymer, an interlayer of un-penetrated PP would arise at the fibre surface. The interphase was postulated to be a semi-interpenetrating network (IPN) between the epoxy resin and the PP so that the relative shear properties of the IPN and interlayer would dictate failure behaviour. The modulus of the allylamine PP was shown by nanoindentation to be larger than that of the acrylic acid PP, indicating a higher crosslink density. This observation supports the diffusion mechanism since the penetration length of the allylamine PP would also be lower [3].

In this paper we examine this hypothesis by studying the interaction of the epoxy resin with the allylamine plasma polymer to establish that an interphasal IPN formed. A model E glass system was developed so that the fracture surfaces could be precisely examined by Time of flight secondary ion mass spectroscopy (ToF SIMS).

2. Experimental

2.1 Materials

Unsize and uncoupled (but water-sized for spinning) E-glass fibres of diameter $14.32 \pm 1.47 \mu\text{m}$ were supplied by Owens Corning Ltd. They were used for the preparation of the 'high' volume fraction composite materials and single filament specimens. Water was used to cool and protect the fibres, during spinning [6]. Therefore, in this work, these fibres will be referred to as unprocessed uncoated fibres (control) to differentiate them from the PP coated ones and those transported through the plasma reactor without the plasma activated. The matrix resin used for the experiment was a mixture of Epikote 828 which is a diglycidyl ether of bisphenol-A (Robnor Resins, UK), 90 phr (parts per hundred resin) 1-methyl-5-norbornene-2, 3-dicarboxylic anhydride (NMA), a curing agent (Huntsman Advanced Materials Ltd, UK), and 1 phr DY062, Benzyl dimethylamine (BDMA), used as the accelerator (Huntsman Advanced Materials Ltd, UK). The resin was cured using the following thermal profile: 2h at 80°C followed by 3h at 120°C with post curing at 150°C for 4h. The monomers utilized for plasma deposition were obtained from Aldrich Chemical Company, UK. The monomers chosen were acrylic acid, allylamine and 1, 7-octadiene with a purity of >99%. They were degassed in 3 freeze-pump-thaw cycles.

2.2 Continuous fibre coating

The plasma reactor was designed to deposit a PP onto the fibre tow continuously, as described elsewhere [7]. The plasma was generated in the plasma reactor by a 13.56 MHz radio frequency power supply at power of 1 W. A low plasma power is effective in retaining the high concentration of amine groups on the surface [8, 9].

During plasma polymerisation, the pressure in the chamber was generally $2 - 3 \times 10^{-2}$ mbar. To deposit coatings of 10 and 15.3 nm, the residence time of the fibres within the reactor barrel was 10 and 15 min respectively. To alleviate any problems associated with the fibre/fibre touch and 'shadowing' within the tow during PP, a blown air source was used to separate the individual filaments within the bundle. During fibre separation, a silicone free release film (Tygavac, UK) was wound onto the glass spool between the layers of fibres. This prevents the fibres from tangling. After the fibres were separated and wound onto the spool, they were loaded into the plasma reactor.

Marks and Jones [7] reported that all fibres in the bundle are completely and coherently coated with the same composition of the PP. The surface chemical composition of the PP deposit was not a function of deposition time. This gives confidence to the conclusion that fibre-separation method can effectively solve problems associated with shadowing, and provide a conformal coating onto all of the individual fibres.

2.3 E-Glass slide coating

E glass slides were prepared by cutting them from a block cast from E glass marbles using a diamond impregnated rotary cutting wheel. The surface was ground and polished to a 1 μm finish. They were cleaned by ultrasonication for 10 minutes in deionised water, hexane and acetone followed by drying and annealing in an oven at 200°C for 2 hours. The slides were then stored in a desiccator.

The E-glass slides were coated with a plasma copolymer of 90% allylamine (AAm) and 10% 1,7-Octadiene (Oct) at a power of 1 W for 20 minutes under a pressure of 3×10^{-3} mbar to deposit a coating with thickness of 20 nm as described elsewhere [3,7]. The slides were cleaned and pre-treated in an O₂-plasma for 15 minutes at a power of 2 W and gas flow rate of 2 cm³_{stp}/min (sccm) prior to plasma polymerisation.

2.4 Model Composites Fabrication

To simulate the interface in a glass fibre composite, a model composite was fabricated in a clean environment for analysis by Time of Flight Secondary Ion Mass Spectrometry (ToF SIMS).

The model fracture comprising of two surfaces was achieved as shown in Figure 1. A release film was used to create a notch for the initiating the fracture of the model composite.

A DGEBA epoxy resin was selected as described in section 2.1. This was sandwiched between the two plasma polymer coated plates and cured at 80°C for 2h followed by 120°C for 3h and post-cured at 150°C for 4h respectively. After curing, the two fracture surfaces were created by applying a manual load as shown in Figure 1. Each surface was used to create a chemical image using ToF SIMS analysis.

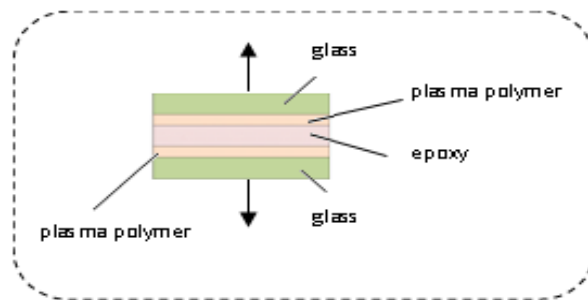


Figure 1. Schematic of the model composite and loading arrangement for the ToF SIMS fractography [10].

2.5. ToF Sims Imaging of Composite Fracture Surfaces

ToF-SIMS was performed on both tows of fibres and composite fracture surfaces using an ION-TOF V secondary ion mass spectrometer with a Bismuth liquid metal ion source providing Bi³⁺ primary ions. The instrument was used in two modes. Firstly high current bunched mode, at 0.12 pA with a cycle time of 100 ns over an area of 150×150 μm and a time of 300 s was used in order to produce high mass resolution spectra. Secondly burst alignment mode with a current of 0.4 pA over an area of 250×250 μm was used to produce high spatial resolution (low mass resolution) images. An electron flood gun was used for charge neutralisation. The maximum primary ion dose was limited to $<5 \times 10^{12}$ ions/cm². The low primary ion doses ensure that the analysis is performed under static conditions and is only sensitive to a depth of material 1–2 nm from the surface. Positive and negative ion data were collected in all cases. In imaging mode a full mass spectrum is generated for each pixel of the image. Compound images for positive and negative ion spectra were then produced by mapping a certain colour channel (red green or blue) to peaks in the mass spectra which could be assigned to a certain constituent of the composite. For example, in the positive ion spectrum peaks at $m/z = 27$ and 40 were used to identify glass since these peaks are indicative of Ca⁺ and Al⁺ ions. The intensities of these peaks were then mapped as red pixels in the compound images. A similar approach was used in the negative ion spectra, but here the red

pixels represent the intensity of the peaks at $m/z = 60$ and 76 since these peaks are indicative of SiO_2^- and SiO_3^- ions respectively. Unfortunately plasma polymerised 1,7-octadiene does not produce any ion fragments which are entirely specific, so only non-specific hydrocarbon ions could be mapped, which would indicate plasma polymerised 1,7-octadiene, but would also be expected to be found from epoxy resin or from hydrocarbon based contamination. The ion assignments for positive and negative spectra are given in Tables 1 and 2. Sections of tow were cut from the beginning and end of the spool of pp coated glass fibre for analysis. An uncoated section of tow was also analysed for control purposes. Because of the need for extreme cleanliness in ToF-SIMS model composite fracture surfaces were obtained from the transverse failure of thin unidirectional coupons with aligned fibres, in flexure and immediately transferred to the to the analysis chamber to minimise contamination.

Table 1. Positive secondary Ions employed for ToF SIMS Fractography of the Glass Fibre Composites[11]

Channel	Material	Mass numbers mapped, m/z	Corresponding ion
Red	Glass	27, 40	Al^+ , Ca^+
Green	Non-specific hydrocarbon	41, 43, 55	C_3H_5^+ , C_3H_7^+ , C_4H_7^+
Blue	Epoxy resin	91, 137	C_7H_7^+ , $\text{C}_9\text{H}_{11}\text{O}^+$

Table 2. Negative secondary Ions employed for ToF SIMS Fractography of the Glass Fibre Composites[11]

Channel	Material	Mass numbers mapped, m/z	Corresponding ion
Red	Glass	60, 76	SiO_2^- , SiO_3^-
Green	Non-specific hydrocarbon	37, 49, 62	C_3H^- , C_4H^- , C_5H_2^-
Blue	Plasma polymerised acrylic acid	71, 113, 145	$\text{C}_3\text{H}_3\text{O}_2^-$, $\text{C}_5\text{H}_5\text{O}_3^-$, $\text{C}_6\text{H}_9\text{O}_4^-$

2.6 ToF Sims Imaging Of Model Fracture Surfaces

The spectra were obtained using an Ion-ToF V, time of flight secondary ion mass spectrometer, (Ion-ToF, Münster, Germany) The base pressure in the analysis chamber was 5×10^{-9} mbar. The primary ion beam was a bismuth liquid metal with an energy of 25 keV which was used as a pulsed ion source. The primary ion beam current was adjusted to 0.22 pA at 100 μs cycle time to provide a high current bunched mode. The total primary ion flux was approximately 5×10^{11} ions cm^{-2} for each acquisition, which is significantly below than the maximum ion dose limit of 1×10^{13} ions cm^{-2} for static SIMS. The spectra were collected from a scanned area of $150 \mu\text{m} \times 150 \mu\text{m}$. The images were obtained from an analysis area of $250 \mu\text{m} \times 250 \mu\text{m}$ which can generate 256×256 pixels. A pulsed low energy electron flood gun was used for charge neutralization.

The IonSpec and IonImage software were used to quantify the spectra and create images from the SIMS data. Secondary ions specific to the three components of the model composite (E-glass, plasma polymer size and epoxy resin) were identified. Table 3 gives the ions selected for the analysis and imaging [10].

3. Results

3.1 Composites

The fracture surface of a composite produced from fibres coated with a pp coating of 1,7-octadiene (Oct) is shown in Fig.2. The fibres are coloured green which indicates the presence of a hydrocarbon coating on their surface. Although the ions employed in the imaging are

non-specific they mainly arise from the Oct plasma polymer. The absence of epoxy resin on the fibres shows that the OctPP coating adheres to the fibre but not to the matrix indicating a weak interface between the pp coating and the matrix. Fig 3 shows an image from the fracture surface of a composite containing the highly functional 100% acrylic acid PP coated fibres. The fibres are mostly devoid of organic matter as shown by the red colour arising from the glass specific ions, in both negative and positive secondary ions. This shows that the matrix resin has reacted with the acrylic acid plasma polymer and that glass/plasma polymer interface is the weakest.

Table 3. Groups of Secondary Positive Ions assigned to the individual components for Tof SIMS imaging of the model fracture surfaces [11]

Channel	Material	Mass numbers mapped	Maximum counts per pixel
Red	AAM PP	28, 30, 56, 70	25
Green	E-glass	27, 40	54
Blue	DGEBA	31, 57, 77, 91, 135, 191	57

In the positive ion image in Fig. 3a the composite was prepared from fibres coated with 100% acrylic acid the blue pixels represent the epoxy resin matrix. It is clear that the resin matrix shown in blue in Fig. 3a is associated with the plasma polymer (blue) in Fig. 3b. The presence of the apparently bare fibres confirms that the interaction between the epoxy and plasma polymer is strong whereas some bare fibre is indicative by the red pixels in both images. The non-specific hydrocarbon (green) appears at the surface of the fibres and may be a remnant of the plasma polymer.

3.2 Model Composite System

A model system was designed to explore the transverse fracture of a glass fibre composite. It consisted of two PP coated E glass slides and the epoxy matrix. The PP was prepared from 90% allylamine/10% 1,7-octadiene to enable more straightforward surface analysis. The ToF-SIMS images from the fracture surfaces of the model composite are shown in Figures 4 and 5. In these images the E-glass surface, plasma polymer and epoxy resin are displayed in green, red or blue pixels respectively. The brightness of the image was dependent on the number of counts so that a group of ions were chosen which were representative of the individual components as shown in Table 4. A colour was assigned to the glass (green), matrix (blue) and PP (red). The maximum number of counts per pixel was adjusted in order to normalize the images for comparison.

For the top fracture surface in Figure 4, (a) shows the overlay image of ions for (glass + PP). It can be observed that the red hue attributed to the plasma polymer is visible. Some green areas indicative of the glass surface are present where 2 small areas have not been fully coated. The overlay image of (glass + epoxy resin) ions in (b) is dominated by the blue colour from the epoxy resin matrix. Image (c) is created from the fracture surface using the (glass + epoxy resin + PP) specific ions. Here the purple colour is indicative of an interpenetrating network between the AAM plasma polymer and DGEBA matrix. However, some patches associated with the glass surface are also present in the fracture surface indicative of an area of poorly coated glass probably associated with some contamination. Thus an interphase has formed between the plasma polymer and the epoxy resin.

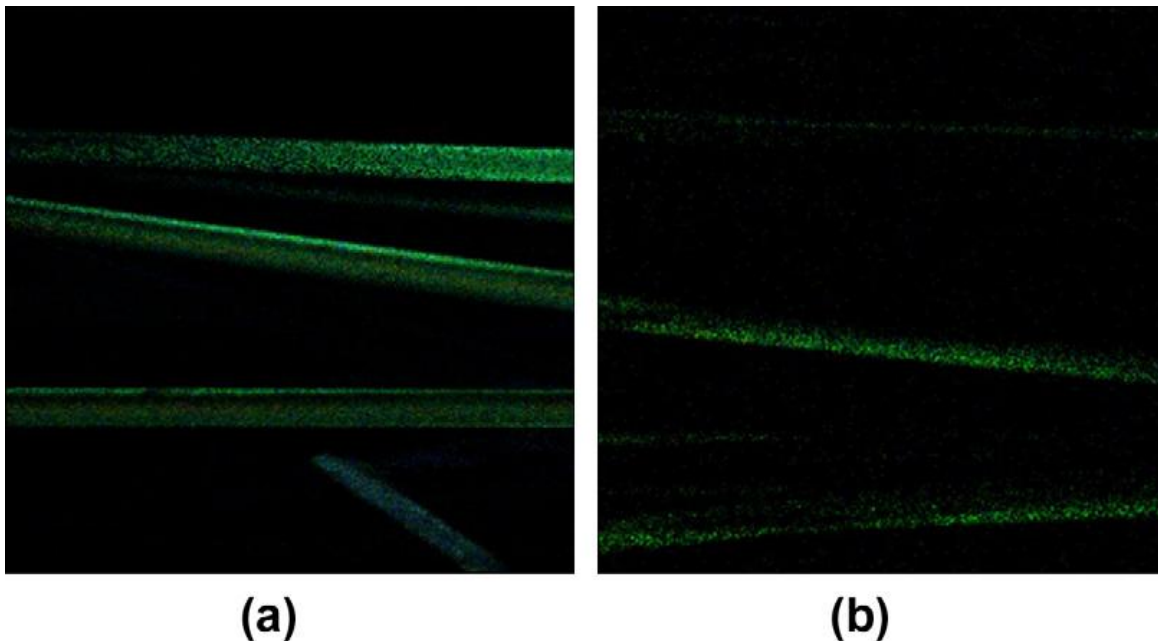


Figure 2 ToF SIMS images of a composite fracture surface from fibres coated with 100% 1,7-Octadiene. (a) positive (b) negative. The fibre surfaces are clearly coated with the non adhering plasma polymer.

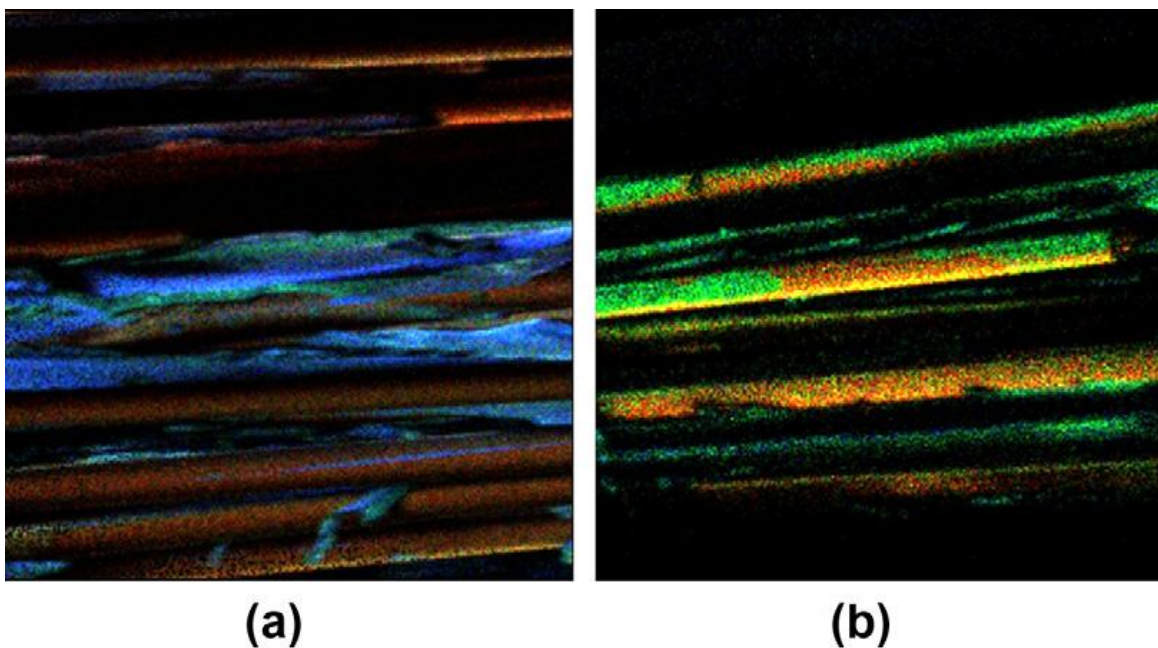


Figure 3 ToF SIMS images of a composite fracture surface from fibres coated with 100% acrylic acid. (a) positive (b) negative.

The crack appears to propagate mainly within the interphase region. The bottom fracture surface, shown in Figure 5, is dominated by ions attributed to E-glass (green pixels) as shown in the overlay images for (a) (glass + plasma polymer) and (b) (glass + epoxy resin). The overlay image (c) of the 3 components is dominated by secondary ions from the E-glass surface. In addition, patches associated with the plasma polymer and epoxy resin interpenetrating network are also present. Thus the crack has propagated through the interphase and at the lower glass surface.

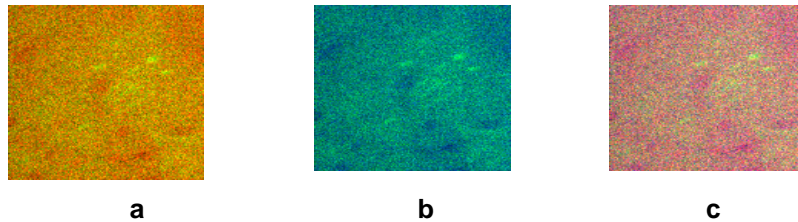


Figure 4 Positive ion overlay images from the top surface of the model fracture prepared from glass slides coated with plasma copolymer from 90% allylamine/10% 1,7-octadiene and epoxy resin (a) glass + plasma polymer (b) glass + epoxy (c) glass + plasma polymer + epoxy

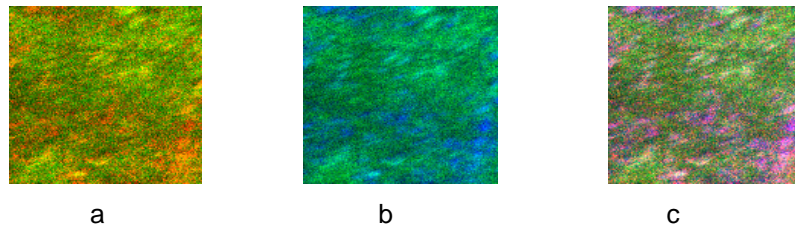


Figure 5 Positive ion overlay Images from the bottom surface of the model fracture prepared from glass slides coated with plasma copolymer from 90% allylamine/10% 1,7-octadiene and epoxy resin (a) glass + plasma polymer (b) glass + epoxy (c) glass + plasma polymer + epoxy

4. Discussion

The ToF SIMS study of the model composite confirms that the ‘epoxy resin’ has penetrated the plasma polymer coated onto the E glass surface to form an interpenetrating network. Furthermore the secondary ions specific to the differing components can be used to image the fracture surfaces of a model composite which shows that the failure crack hugs the glass surface. This confirms the observations reported for the fracture of fibre composites in section 3.1. The bond between the plasma polymer and the E glass surface is observed to be weaker than that between the plasma polymer and the epoxy resin matrix. This study also supports the model of the interphase which was postulated to explain the change in interlaminar shear strength with plasma polymer thickness reported by Liu et al. [3].

In a future paper we will report a study of the penetration length scale which demonstrates that an interlayer of plasma polymer can form at greater thicknesses of plasma polymer size [3]. The unanswered question is whether the individual components of the ‘epoxy resin’ diffuse independently to provide a preferential reaction with the amine groups on the plasma polymer. The curing mechanism involves the alternate copolymerization of the anhydride and epoxy monomer initiated by the tertiary amine accelerator so that this will be in competition with the direct reaction of the amine groups in the plasma polymer size and the epoxy monomer. This may partly explain the differences between the performance of the composites with allylamine PP and acrylic acid PP fibre sizings and the differing effects of sizing thickness.

5. Conclusions

The hypothesis that an interphase forms from the interaction of the plasma polymer fibre-size and the ‘epoxy resin’ matrix has been confirmed. The ToF SIMS fractography of unidirectional fibre composites shows that the interaction between a non-functional plasma polymer (Oct) and epoxy resin is weak relative to that between the PP and the glass surface whereas with a reactive plasma polymer the situation is reversed with failure occurring at the glass surface. The penetration of the plasma polymer by the epoxy resin during manufacture

to form a semi-interpenetrating network was implicit in the fracture surfaces of fibre composites. Therefore, E glass slides with a plasma polymer of allylamine and 1, 7-octadiene as the functional size have been used to model the formation of an interphase. We have shown that an interpenetrating network forms between the epoxy resin matrix and the plasma polymer coating and that the interface between the glass and the plasma polymer dominates the failure crack path. The formation of an IPN ensures that the bond between the matrix resin and the plasma polymer coating is strong. However the extent of diffusion of the matrix resin into the PP determines if an 'interlayer' of un-penetrated coating remains at the fibre surface. In this case the stress transfer efficiency at the interface is dominated by the properties of the nanoscale plasma polymer. The interphase may have a complex layered structure if the thickness of the coating exceeds the diffusion length.

6. Acknowledgements

We thank Thailand Institute of Scientific and Technological Research and Royal Thai Government, EPSRC, University of Sheffield and Department of Materials Science and Engineering for financial support.

References

- [1]. Kettle A.P., Beck A.J., O'Toole L., Jones F.R., Short R.D., Plasma polymerization for molecular engineering of carbon – fibre surfaces for optimized composites, *Composites Science and Technology*, **57**, pp. 1023 – 1032.(1997).
- [2]. Kettle A.P., Jones F.R., Alexander M.R., Short R.D., Stollenwerk M., Zabold J., Michaeli W., Wu W., Jacobs E., Verpoest I., Experimental evaluation of the interphase region in carbon fibre composites with plasma polymerised coatings, *Composites Part A: Applied Science and Manufacturing*, **29A**, pp. 241 – 250(1998).
- [3]. Liu Z., Zhao F.M., Jones F.R., Optimising the interfacial response of glass fibre composites with a functional nanoscale plasma polymer coating. *Composites Science and Technology*, **68**, pp 3161 – 3170(2008).
- [4]. Drzal L.T., Rich M.J., Lloyd P.F., Adhesion of Graphite Fibres to Epoxy Matrices: 1.The Role of Fibre Surface Treatment, *Journal of Adhesion*, **16**, pp. 1–30. (1983)
- [5]. Maeder E., Moos E., Karger-Kocsis J., Role of film formers in glass fibre reinforced polypropylene – new insights and relation to mechanical properties, *Composites: Part A*, **32**, pp. 631 – 639. 2001
- [6]. Wu H.F., Dwight D.W., Huff N.T., Effects of silane coupling agents on the interphase and performance of glass-fibre-reinforced polymer composites, *Composites Science and Technology*, **57**, pp. 975 – 983. (1997)
- [7]. Marks D.J., Jones F.R., Plasma polymerised coatings for engineered interfaces for enhanced composite performance, *Composite. Part A: applied science and manufacturing*, **33**, pp 1293 – 1302 (2002).
- [8]. Beck A.J., Jones F.R., Short R.D., Plasma copolymerization as a route to the fabrication of new surfaces with controlled amounts of specific chemical functionality, *Polymer*, **37**, pp.5537 – 5539 (1996).
- [9]. Lopattananon N., Hayes S.A., Jones F.R., Stress transfer function for interface assessment in composites using plasma copolymer functionalized carbon fibres, *Journal of Adhesion*, **78**, pp. 313 – 350 (2002).
- [10]. Swait T.J., Whittle T., Soutis C., Jones F.R., Identification of interfacial and interphasal failure in composites of plasma polymer coated fibres, *Composites part A*, **41**, pp.1047-1055 (2010).
- [11]. Photjanataree P., Liu Z., Jones F.R., The role of a nanoscale interphase from plasma polymers on the micromechanics of fiber composites, *Macromol.Mater.Eng*, DOI:10.1002/mame.201100341 (2012).